Narrow chaotic compound autoionizing states in atomic spectra

V. V. Flambaum, A. A. Gribakina, and G. F. Gribakin
School of Physics, University of New South Wales, Sydney 2052, Australia
(Received 12 December 1995)

Simultaneous excitation of several valence electrons in atoms gives rise to a dense spectrum of compound autoionizing states (AIS). These states are almost chaotic superpositions of large numbers of many-electron basis states built of single-electron orbitals. The mean level spacing D between such states is very small (e.g., $D<0.01$ eV for the numerical example of $J^{\pi}=4^{-}$ states of Ce just above the ionization threshold). The autoionization widths of these states estimated by perturbations, $\gamma=2\pi|W|^2$, where W is the Coulomb matrix element coupling the AIS to the continuum, are also small, but comparable with D in magnitude: $\gamma\sim D$. Hence the nonperturbative interaction of AIS with each other via the continuum is very essential. It suppresses greatly the widths of the autoionizing resonances ($\Gamma\simeq D^2/3\gamma\ll D$), and leads to the emergence of a ''collective'' doorway state which accumulates a large share of the total width. This state is in essence a modified single-particle continuum decoupled from the resonances due to its large width. Narrow compound AIS should be a common feature of atomic spectra at energies sufficient for excitation of several electrons above the ground-state configuration. The narrow resonances can be observed as peaks in the photoabsorption, or, in electron-ion scattering, as Fano-type profiles on the background provided by the wide doorway-state resonance. It is also shown that the statistics of electromagnetic and autoionization amplitudes involving compound states are close to Gaussian. [S1050-2947(96)07208-3]

PACS number(s): 32.80.Dz, 31.50.+w, 34.80.−i

I. INTRODUCTION

It is well known that simultaneous excitation of several atomic electrons into discrete states can produce autoionizing states (AIS's) seen as narrow resonances in the continuous spectrum of the system at energies above the ionization threshold. In atoms with two valence electrons, such as helium, or alkaline earths, the spectrum of such resonances remains relatively simple. It essentially consists of Rydberg-like series converging to excited states of the positive ion. These states can be classified using single-electron or some other quantum numbers. If the number of excited electrons is greater than two, the number of many-electron states that can be formed from them rapidly increases (exponentially, with the number of excited electrons), and the structure of such states is of much greater complexity. This behavior follows from simple combinatorial consideration, and is realized in excited states of rare-earth atoms, where several open shells exist in the immediate vicinity of the ground state.

Indeed, the extreme complexity of the rare-earth atoms spectra at excitation energies of a few eV, well below the ionization threshold, can be seen from the level tables [1]. The complexity becomes even greater in the spectra of lanthanides and actinides just below the ionization threshold, and the associated difficulties one encounters trying to identify Rydberg series of levels are very well known to experimentalists (see, e.g., [2] and [3], where the first observation of Rydberg series in any actinide was made for U). Similar states can be formed in other atoms with simpler electron structure at higher excitation energies (see, e.g., the experimental $4p$-photoabsorption spectrum of Sr in [4], and the discussion and references therein). In any case, the density of such excited states is very large, and the mean level spacing D is very small (by D we understand the mean spacing between the levels of the same symmetry, i.e., of the same total angular momentum and parity J^{π}). Clearly, D is energy dependent: the higher the energy E, the larger the density of states $\rho(E)$, and the smaller the value of $D=\rho^{-1}$. For example, in the independent-particle model one obtains $\rho(E)=\rho_0\exp(a\sqrt{E})$ [5], and the experimental spectra of rare-earth atoms were shown to be in agreement with this dependence [6].

The small value of D has immediate physical implications for these many-electron states. Suppose that one uses a basis of some single-electron orbitals to construct many-electron basis states $|\Phi_k\rangle$. The states $|\Phi_k\rangle$ can be taken as single-determinant states corresponding to certain electron configurations, or constructed from them through some coupling scheme to have a definite J value. The true atomic eigenstates

$$|A^*i\rangle=\sum_k C_{ik}|\Phi_k\rangle \quad \left(\sum_k C_{ik}^2=1\right) \tag{1}$$

are obtained by diagonalizing the Hamiltonian matrix $H_{ik}\equiv\langle\Phi_i|H|\Phi_k\rangle$. The coefficients C_{ik} describe mixing of the basis states by the residual Coulomb interaction. The number of basis states $|\Phi_k\rangle$ formed by distributing several electrons among a few open orbitals is large, and the mean spacing between the basis-state energies H_{kk} (this spacing is $\sim D$, if the basis states with definite J are used) is smaller than the typical value V of the off-diagonal matrix element H_{ik}. In this situation the basis states are strongly mixed by the perturbation. Apart from several lowest levels, which can be described by a single dominant electron configuration, each of the eigenstates is a superposition of a large number of basis states. This strong mixing takes place within a certain energy range $\Gamma_{\rm spr}$ called the spreading width since it characterizes the spread of the eigenstates to which a given basis state contributes noticeably (in simple models with

constant off-diagonal matrix elements the spreading width is obtained as $\Gamma_{\rm spr}=2\pi V^2/D$; see, e.g., [5]). By the same token, one can estimate the number of principal components, i.e., those largely contributing to the sum (1), as $N\sim\Gamma_{\rm spr}/D$. The coefficients C_{ik} corresponding to the principal components have typical values $|C_{ik}|\sim 1/\sqrt{N}$. Their statistics are close to those of independent random variables, and become Gaussian when the mixing is complete. The notion of electronic configuration becomes meaningless for these eigenstates, since even the single-electron orbital occupancies are very far from integer, and only the total angular momentum and parity remain good quantum numbers. One can view these features as signatures of quantum chaos in the system.

Such a picture is commonly used to describe compound resonances in nuclei. It has recently been shown to be applicable to excited states of the rare-earth atom of Ce at $E\gtrsim 2$ eV [7]. The model configuration-interaction calculations performed in [7] produced a value of $\Gamma_{\rm spr}\sim 2$ eV, and demonstrated the existence of a dense spectrum of compound ''chaotic'' excited states with $N\gtrsim 100$ ($D\sim 0.01$ eV). In nuclei compound states are usually observed as narrow resonances in low-energy neutron scattering. The energy of the incident neutron with respect to the ground state of the compound nucleus (the neutron threshold, which is about 8 MeV) is shared in these states by a large number of valence nucleons. The number of these multiply excited states is enormous, and the level spacing D can be as small as 1 eV, whereas the typical nuclear energy scale is 1 MeV. The corresponding number of principal components in nuclear compound states can reach $N\sim 10^6$. Our present study was initiated by the following question: Can one observe analogous dense spectra of compound excited states above the ionization threshold in atoms?

In order to answer this question it is necessary to estimate the widths of compound AIS's and compare them with the level spacing D. The width as given by perturbation theory is

$$\gamma_i=2\pi|\langle A^+\varepsilon l|W|A^*i\rangle|^2, \tag{2}$$

where we assume that the decay is dominated by a single channel, and W is the Coulomb interaction between atomic electrons. Contrary to the compound AIS $|A^*i\rangle$, the final state $\langle A^+\varepsilon l|$, which describes the ion in the ground state and the continuum electron, is relatively simple; thus it has a well-defined electron configuration. By analogy with estimates of matrix elements involving nuclear compound states [8], we obtain

$$\langle A^+\varepsilon l|W|A^*i\rangle=\sum_k \langle A^+\varepsilon l|W|\Phi_k\rangle C_{ik}\sim W_0\left(\frac{q}{N}\right)^{1/2}, \tag{3}$$

where W_0 is a typical matrix element between ''simple'' many-electron states (essentially, a two-body Coulomb matrix element); q is the number of nonzero items in the sum, given by such k that Φ_k differs from $A^+\varepsilon l$ by no more than two single-electron states, and the signs of the items are supposed to be random due to randomness of C_{ik}. Being the sum of uncorrelated random variables, the matrix element (3) should obey Gaussian statistics.

If the excited atomic state involves more than two valence electrons, then $q\ll N$, and the decay matrix element for the compound AIS is suppressed with respect to that of a ''simple'' two-electron AIS. The estimate for the width (2) then reads

$$\gamma\sim 2\pi W_0^2\frac{q}{N}\sim\frac{2\pi W_0^2 q}{\Gamma_{\rm spr}}D, \tag{4}$$

where $2\pi W_0^2$ can be considered as the width of a simple low-lying two-electron AIS (for example, the $3d5p\ ^1P_1$ state of Ca, which lies 0.46 eV above the threshold and has a width of about 0.07 eV; see, e.g., [9]). Estimate (4) shows that the widths of compound AIS's are proportional to the level spacing. Combining the above quoted value of the width for Ca with a plausible yet arbitrary $q=10$ and $\Gamma_{\rm spr}\simeq 2$ eV, we obtain $\gamma\sim 0.5D$. If one takes into account fluctuations of the widths and positions of the compound AIS's, this estimate would suggest a picture of a dense spectrum of overlapping resonances in the atomic continuum.

However, in the situation when the widths are of the order of the level spacing the perturbation estimate (2) becomes invalid, and the interaction of the discrete states with each other via the continuum should be taken into account in all orders. The problem of n discrete levels interacting with one continuum has been known for a long time [10]. In the situation when $\gamma_i\ll D$, a succession of asymmetric resonance contours (Fano profiles) is observed, for instance, in the photoabsorption cross section. The profiles are characterized by the width $\Gamma_i\approx\gamma_i$ and the asymmetry parameter

$$q_i\approx\frac{\langle A^*i|Q|A\rangle}{\pi\langle A^+\varepsilon l|Q|A\rangle\langle A^*i|W|A^+\varepsilon l\rangle}, \tag{5}$$

where Q is the transition operator (the electric dipole), $|A\rangle$ is the initial state of the atom, and the admixture of the continuum states to the AIS has been neglected (otherwise the numerator of q_i has to be modified). The positions of the resonances are slightly shifted with respect to the original energies of the AIS. In the opposite situation $\gamma_i\gg D$ one observes a remarkable transformation of the spectrum [11–16]. If the number of levels interacting with the continuum is finite, a ''collective'' state is pushed away into the complex energy plane, collecting most of the total width $\Gamma=\Sigma_i\gamma_i$. Other $n-1$ resonances are strongly shifted from their unperturbed positions, and their widths are greatly suppressed: $\Gamma_i\sim D^2/3\gamma\ll D$, where γ is the average value of γ_i (see below). The latter means that $n-1$ narrow resonances become almost decoupled from the continuum.

One can obtain a simple physical picture of narrowing in the following model. Suppose that there is a *doorway* state $|c\rangle$ which is strongly coupled to the continuum, i.e., has a large width Γ_c, and that the other discrete states $|i\rangle$ are coupled to the continuum via this state. Their widths calculated by perturbations are

$$\Gamma_i=\frac{\Gamma_c}{(E-E_c)^2+\Gamma_c^2/4}|\langle c|W|i\rangle|^2. \tag{6}$$

If the states in question are within the width of the doorway, $|E-E_c|<\Gamma_c$, the widths Γ_i are inversely proportional to Γ_c. Similarly, when a short-lived ''collective'' state is formed in the spectrum, the capture from the continuum into

other discrete states proceeds via this state. Thus the collective state is in fact just a modified single-particle continuum (see Sec. II C), or, in other words, a doorway state.

In nuclei at energies just above the neutron threshold, the perturbative situation ($\gamma \ll D$) is realized. Besides the statistical suppression of the widths, expressed by (4), they are also suppressed by a kinematical factor kR (for s-wave resonances). Here k is the wave vector of the neutron, and R is the nuclear radius. With the excitation energy increasing, the widths also increase, due to both the kinematical factor and the contribution of other decay channels. So, by the time when $\gamma \sim D$, the single-decay-channel approximation is no longer valid, and the interesting second regime of width suppression is not observed.

In atoms, however, the outgoing electron is moving in the Coulomb field of the ionic residue. Hence the kinematical suppression factor does not work (although it should manifest for autodetaching negative ion states). Then, if the relation $\gamma \gtrsim D$ takes place, either for dynamical reasons, or because of a local fluctuation, the second regime will take over. The observed spectrum will depend on the physical process involved. Thus in the photoabsorption measurement the narrow resonances will be the main feature of spectrum, since the oscillator strength of the continuumlike broad collective (doorway) resonance is roughly $1/n$ of the total oscillator strength. However, in electron-ion scattering the doorway-state resonance may become the dominant feature of the cross section, because of its strong coupling to the continuum. At sufficient resolution, however, narrow resonances will be observed as sharp cuts slicing the broad-scale background.

In Sec. II we give a theoretical description of the phenomenon, and derive some analytical results for model cases. In Sec. III a more realistic model of compound AIS's in atomic Ce is considered numerically using the configuration-interaction (CI) method. This allows us to check that our understanding of the effect is correct and gives an insight into the role of fluctuations. Section IV summarizes the results and poses some general questions about the structure of the atomic continuum.

II. THEORY

In this section we present a very compact derivation of the formalism describing a set of levels embedded in and interacting with a continuum, and survey the effects this interaction produces on the widths of the resonances in the spectrum.

A. Basic equations

Let us consider a particular process where one can study the interaction of AIS's with the continuum, namely, photoionization. Suppose the atomic system is initially in some state g. After the absorption of a photon the system can be transferred either to the state ε in the continuum, or to one of the discrete state i, which will decay into the ε state due to the residual interaction W. In addition, the interaction with the continuum can result in transitions between different discrete states. The amplitude of the photoionization can be presented graphically as a perturbation theory series:

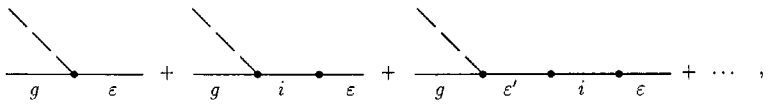

(7)

where summation or integration over the intermediate states (i,ε') is assumed. Analytically, the contribution of diagrams (7) can be written as follows:

$$\langle \varepsilon|\hat{d}|g\rangle + \sum_i \frac{\langle \varepsilon|W|i\rangle\langle i|\hat{d}|g\rangle}{E-E_i} + \sum_i \int \frac{\langle \varepsilon|W|i\rangle\langle i|W|\varepsilon'\rangle\langle \varepsilon'|\hat{d}|g\rangle d\varepsilon'}{(E-\varepsilon'+i\delta)(E-E_i)} + \cdots, \tag{8}$$

where $\langle \varepsilon|\hat{d}|g\rangle \equiv d$ and $\langle i|\hat{d}|g\rangle \equiv Q_i$ are the dipole amplitudes of the electromagnetic transitions into the continuum and the state i, respectively; E_i are the energies of the discrete states; and E is the energy of the system ($E=E_g+\hbar\omega$). Introducing $\chi_{ij}=(E-E_i)^{-1}\delta_{ij}$ and $W_i=\langle i|W|\varepsilon\rangle$, we can write the expression for the amplitude using matrix notation:

$$A(E) = d + W^\dagger \chi Q + W^\dagger \chi \widetilde{Q} + W^\dagger \chi \Sigma \chi Q + W^\dagger \chi \Sigma \chi \widetilde{Q} + \cdots, \tag{9}$$

where

$$\widetilde{Q}_i = \int \frac{\langle i|W|\varepsilon'\rangle\langle \varepsilon'|\hat{d}|g\rangle}{E-\varepsilon'+i\delta} d\varepsilon' \tag{10}$$

is the dipole amplitude of the $g \to i$ excitation via the continuum, and the matrix

$$\Sigma_{ij} = \int \frac{\langle i|W|\varepsilon'\rangle\langle \varepsilon'|W|j\rangle}{E-\varepsilon'+i\delta} d\varepsilon' \tag{11}$$

describes the interaction of the discrete states via the continuum. Summing the matrix geometric series in (9), we obtain

$$A(E)=d+W^{\dagger}(\Delta-\Sigma)^{-1}[Q+\tilde{Q}], \tag{12}$$

where $\Delta=\chi^{-1}$, i.e., $\Delta_{ij}=(E-E_i)\delta_{ij}$, and the second term on the right-hand side corresponds to the excitations of the AIS modified by the interaction with the continuum. This amplitude is equivalent to the solution of the Fano problem of n discrete levels interacting with a continuum [10]. There are generalization of Fano's theory to the many-continua case [11], which can also be done using the present formalism (see Appendix B).

Poles of the amplitude $A(E)$ correspond to resonances in the spectrum. The positions of the poles are determined by $(\Delta-\Sigma)^{-1}\to\infty$, which is equivalent to $\det(\Delta-\Sigma)=0$. The values of E which satisfy this equation are, in fact, eigenvalues of the matrix $E_i\delta_{ij}+\Sigma_{ij}$,

$$E_iC_i+\sum_j \Sigma_{ij}C_j=EC_i. \tag{13}$$

Using the relation $(E-\varepsilon+i\delta)^{-1}=(E-\varepsilon)^{-1}-i\pi\delta(\varepsilon-E)$, we can present (11) as

$$\Sigma_{ij}=\int \frac{\langle i|W|\varepsilon'\rangle\langle\varepsilon'|W|j\rangle}{E-\varepsilon'}d\varepsilon'-i\pi\langle i|W|\varepsilon\rangle\langle\varepsilon|W|j\rangle, \tag{14}$$

where the integral is understood in the principal value sense, and the continuous spectrum state $|\varepsilon\rangle$ corresponds to the energy E at which Σ_{ij} is calculated. The first term on the right-hand side of (14) is Hermitian. It shifts the positions of AIS's along the real axis with respect to the unperturbed energies E_i. The second, anti-Hermitian term shifts the eigenvalues of (13) into the complex plane, thus determining the widths of the AIS's. For example, in the perturbation theory regime when the interaction with the continuum is small, the width of the AIS i is given by $-2\,\mathrm{Im}\Sigma_{ii}=2\pi|\langle i|W|\varepsilon\rangle|^2\equiv\gamma_i$.

In the present work we are interested in the evolution of the widths, and below we neglect the first term in (14). This approximation is quite reasonable if the matrix elements in the integrand in Eq. (14) depend weakly on energy, making the principal value of the integral close to zero [17]. If ε is the energy of the autoionizing electron moving in the field of the ion, the matrix element $\langle\varepsilon|W|i\rangle$ is indeed constant at small ε due to the Coulomb asymptotic of the ionic potential [18] [the continuous spectrum wave functions are normalized to $\delta(\varepsilon-\varepsilon')$]. On the other hand, one can always diagonalize the Hermitian part of $(E_i\delta_{ij}+\Sigma_{ij})$ first, and then study the widths of AIS in the new basis, in which Σ_{ij} is anti-Hermitian. We must add that, strictly speaking, the matrix Σ_{ij} is energy dependent. Therefore, Eq. (13) is not a conventional eigenvalue problem. However, the characteristic scale of this energy dependence ($\Delta E\sim I$ for atoms) is much greater than the mean level spacing D, and hence can be neglected when studying the interaction of nearby levels.

B. Positions of resonances

The anti-Hermitian part of Σ_{ij}, Eq. (14), is separable ($\Sigma_{ij}=-i\pi W_iW_j^*$). It is well known [19] that for a separable potential the eigenvalue problem (13) can be reduced to a simple algebraic equation

$$1+\frac{i}{2}\sum_i \frac{\gamma_i}{E-E_i}=0 \tag{15}$$

whose roots are determined by the unperturbed energies E_i and the diagonal matrix elements $\Sigma_{ii}\equiv-(i/2)\gamma_i$. If we treat E as a complex variable explicitly, $E\to E-i\Gamma/2$, Eq. (15) is equivalent to the following two equations:

$$\sum_i \frac{\gamma_i(E-E_i)}{(E-E_i)^2+\Gamma^2/4}=0, \tag{16a}$$

$$\frac{\Gamma}{4}\sum_i \frac{\gamma_i}{(E-E_i)^2+\Gamma^2/4}=1. \tag{16b}$$

It is easy to check that in the limit $\gamma_i\ll D$ Eq. (15) or Eqs. (16) have a solution $E=E_i+O(\gamma^2/D)$, $\Gamma_i=\gamma_i+O(\gamma^3/D^2)$ (perturbation theory limit). Of course, these equations cannot be solved for arbitrary E_i,γ_i. There was quite a number of papers which studied the properties of their solutions, both analytically and numerically [13–16,20,21]. In what follows we examine several model cases, and in Sec. III present the results of a realistic calculation for the cerium atom.

1. The picket-fence model

Let us first consider the simplest case of an infinite equidistant spectrum, $E_{i+1}-E_i=D=\mathrm{const}$, with identical coupling to the continuum, $\gamma_i=\gamma$ (see also [20]). It is obvious that in this case the first equation (16a) has a solution $E=E_i$. The sum in the left-hand side of (16b) is then

$$\sum_{k=-\infty}^{\infty}\frac{\gamma}{(kD)^2+\Gamma^2/4}=\gamma\left(\frac{4}{\Gamma^2}+\frac{2}{D^2}\sum_{k=1}^{\infty}\frac{1}{k^2+(\Gamma/2D)^2}\right).$$

Making use of the formula $\coth\pi x=(1/\pi x)+(2x/\pi)\Sigma_{k=1}^{\infty}1/(x^2+k^2)$ [22], from Eq.(16b) we obtain:

$$\Gamma=\frac{2D}{\pi}\tanh^{-1}\frac{\pi\gamma}{2D}. \tag{17}$$

If γ is small ($\gamma\ll D,\tanh^{-1}z\sim z$), Eq. (17) yields $\Gamma\simeq\gamma$ (this is the perturbation theory limit). It is clear that Eq. (17) has a solution only for $\gamma<2D/\pi$ and for $\gamma=2D/\pi$ the widths Γ becomes infinite. In the model with a finite number of levels n this critical point corresponds to the emergence of a collective state whose width tends to infinity at $n\to\infty$ (see below; also see Appendix A).

However, in the equidistant model, Eq. (16a) has another solution, $E=E_i+D/2$. In this case the left-hand side of (16b) is transformed with the help of $\tanh(\pi x/2)=(4x/\pi)\Sigma_{k=1}^{\infty}1/[(2k-1)^2+x^2]$ [22], giving

$$\frac{\Gamma}{4}\sum_{k=-\infty}^{\infty}\frac{\gamma}{(D/2-kD)^2+\Gamma^2/4}=\frac{\gamma\pi}{2D}\tanh\frac{\pi\Gamma}{2D},$$

and Eq. (16b) yields

$$\Gamma=\frac{2D}{\pi}\tanh^{-1}\frac{2D}{\pi\gamma}. \tag{18}$$

This solution is valid for $\gamma > 2D/\pi$. For $\gamma \gg D$ the width is given by

$$\Gamma \simeq \frac{4D^2}{\pi^2 \gamma} \ll D. \tag{19}$$

Thus in the case of strongly interacting resonances the widths are suppressed, and the effect of narrowing takes place.

2. Finite number of levels

If we consider a finite number of levels n, then the total width $\Sigma_{i=1}^{n} \Gamma_i$ is given by $-2\,\mathrm{Im}\,\mathrm{Tr}(\Sigma) = \Sigma_{i=1}^{n} \gamma_i$. For $\gamma_i \ll D$ perturbation theory gives the same result, $\Gamma_i = \gamma_i$, as for the infinite number of levels. On the other hand, for $\gamma_i \gtrsim D$ it is not possible to observe narrowing of *all* resonances, since this will contradict $\Sigma_i \Gamma_i = \Sigma_i \gamma_i$. Nevertheless, it is easy to see that in this regime all resonances are narrowed, except one, which accumulates almost all width. Let us calculate the width and the position of this collective state for $\gamma_i \gg D$. From Eq. (16b) one can obtain

$$\Gamma = \sum_i \frac{\gamma_i}{1 + \dfrac{4(E-E_i)^2}{\Gamma^2}} = \sum_i \gamma_i - \sum_i \frac{4(E-E_i)^2 \gamma_i}{\Gamma^2} + \cdots$$

$$\simeq \sum_i \gamma_i - \frac{4\Sigma_i (E-E_i)^2 \gamma_i}{(\Sigma_i \gamma_i)^2}, \tag{20}$$

where we used $\Gamma^2 \gg (E-E_i)^2$, and replaced Γ in the second term by the leading contribution, $\Sigma_i \gamma_i$ (note that the width of the collective state can be calculated on a much weaker condition $\Gamma \gg D$, Appendix A). Indeed, in this regime the collective state width (20) is almost equal to the total width of all resonances. The energy E of the collective state can be easily obtained from (16a):

$$E = \sum_i \frac{\gamma_i E_i}{1 + \dfrac{4(E-E_i)^2}{\Gamma^2}} \left[\sum_i \frac{\gamma_i}{1 + \dfrac{4(E-E_i)^2}{\Gamma^2}} \right]^{-1} \simeq \frac{\Sigma_i E_i \gamma_i}{\Sigma_i \gamma_i}. \tag{21}$$

This energy is the weighted average of the unperturbed energies. If E_i are uniformly distributed over some energy interval and γ_i are random variables (e.g., with a Porter-Thomas distribution), then E will be located roughly in the middle of the interval. The total width of the rest $n-1$ resonances is given by the second term in (20); therefore, their mean width is

$$\overline{\Gamma_k} = \frac{1}{n-1} \frac{4\Sigma_i (E-E_i)^2 \gamma_i}{(\Sigma_i \gamma_i)^2}. \tag{22}$$

Introducing $\overline{\gamma} = (1/n)\Sigma_i \gamma_i$, and replacing the sum in the numerator by the integral

$$\sum_i (E-E_i)^2 \gamma_i \approx \int_{E-nD/2}^{E+nD/2} \overline{\gamma} (E-E_i)^2 \frac{dE_i}{D} = \frac{\overline{\gamma} n^3 D^2}{12},$$

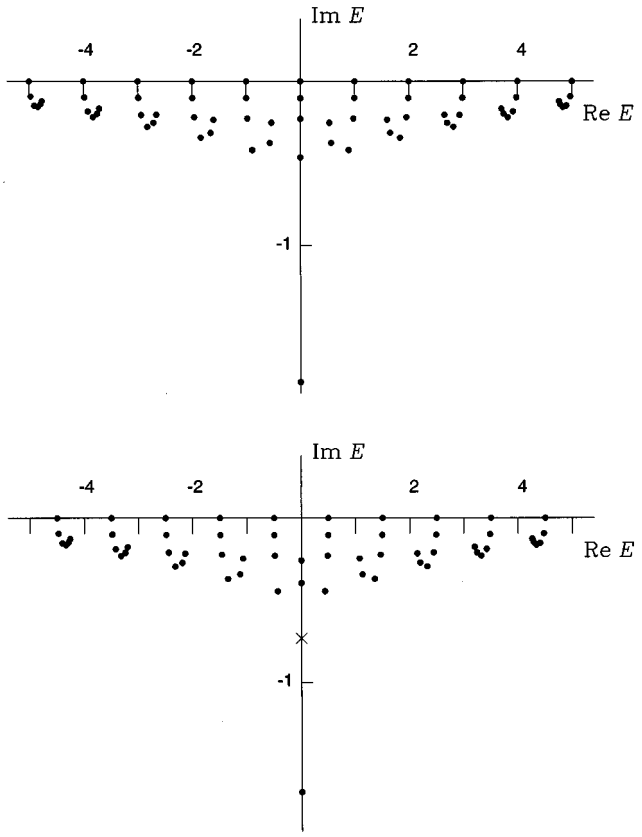

FIG. 1. Behavior of the roots of $1 + (i/2)\Sigma_i \gamma_i/(E-E_i) = 0$ for $n = 11$ (upper graph) and $n = 10$ (lower graph), as a function of γ/D: $\gamma/D = 0$, 0.2, 0.4, 0.6, 0.8, and 1. The cross mark in the lower graph shows the position of the degenerate level at $\gamma/D \approx 0.718$.

we obtain the estimate

$$\overline{\Gamma_k} \simeq \frac{D^2}{3\gamma} \approx 0.33 \frac{D^2}{\overline{\gamma}}. \tag{23}$$

Note that this result is rather close to the one of the picket-fence model [Eq. (19)], $\Gamma \approx 0.40 D^2/\gamma$ (the difference between the two numerical factors is discussed below).

3. Numerical example

Let us illustrate the effects considered above by solving Eq. (15) numerically for a finite number of equidistant levels with identical coupling to the continuum. Figure 1 shows the roots of Eq. (15) for $n = 10$ and 11, and $D = 1$, on the complex plane for different γ: $\gamma = 0$, 0.2, 0.4, 0.6, 0.8, and 1. It be seen on the graph that for the lowest nonzero value $\gamma = 0.2$ the system is in the perturbation theory regime [$\Gamma \simeq \gamma, \mathrm{Im}E = -(\Gamma/2) \simeq -0.1$]. For $\gamma = 0.4$ the perturbation theory is still valid for the levels in the middle of the spectrum, whereas it breaks down for the levels at the edges (see Appendix A). For $\gamma = 0.6$ the widths reach their maxima, and beyond this value, for $\gamma = 0.8$ and 1, the regime of narrowing takes over. For these values of γ all resonances are getting narrower except the collective state, which rapidly takes off into the complex plane [$\Gamma \approx nD/\tan(D/\gamma)$, Appendix A]. Let

us note that the value 0.6 is close to the critical value $2D/\pi \simeq 0.64$ for an infinite number of levels.

For an odd number of levels the collective state originates from the central state whose width increases dramatically for $\gamma > 0.6$ (see the upper graph). For an even number of levels the formation of the collective state proceeds differently. The two resonances closest to the center move toward each other, and for $\gamma \simeq 0.718$ (cross mark in Fig. 1) form a degenerate state. For larger γ one of the levels returns to the real axis and the other one moves in the opposite direction.

Figure 1 shows that for $\gamma > 0.6$ the energies of resonances around the middle of the spectrum move toward the centers of intervals between unperturbed levels. This behavior is in agreement with the results of the infinite picket-fence model in the regime of narrowing [see above Eq. (18)]. Thus $n \sim 10$ is large enough for the picket-fence model to be valid in the central part of the spectrum. The widths of these levels are larger than those of the levels at the edges. Therefore, the mean value of the width is smaller than the widths of the central levels for which the picket-fence estimate (19) is valid. This explains the difference between the numerical factors in Eqs. (19) and (23).

C. Nature of the collective (doorway) state and narrowing

In order to obtain a better understanding of the nature of the collective state, let us calculate the corresponding eigenvector. Inserting the anti-Hermitian separable Σ_{ij} (as in Sec. II B) into Eq. (13), one obtains

$$C_i = -\frac{i\pi q W_i}{E - E_i}, \quad q = \sum_j W_j^* C_j . \tag{24}$$

If we consider the collective state which emerges in the nonperturbative regime, $E = E_c - (i/2)\Gamma_c$,

$$E_c = \frac{\Sigma_i E_i \gamma_i}{\Sigma_i \gamma_i}, \quad \Gamma_c = \sum_i \gamma_i , \tag{25}$$

the energy difference $E_c - E_i$ can be neglected in the denominator of Eq. (24), and the corresponding eigenvector is

$$|\Psi_c\rangle = \sum_i C_i |i\rangle \approx \frac{2\pi q}{\Gamma_c} \sum_i |i\rangle\langle i|W|\varepsilon\rangle . \tag{26}$$

In applications the continuous spectrum states $|\varepsilon\rangle$ usually refer to the electron (nucleon) moving in the field of the atomic (nuclear) residue; i.e., they are single-particle excitations. From this point of view (26) is just a projection of the modified continuous spectrum state $W|\varepsilon\rangle$ onto the subspace of discrete excitations. Thereby, the ''collective'' state is essentially a single-particle doorway-state resonance decoupled from the rest of the quasidiscrete spectrum of multiparticle excitations due to the large value of its width, which couples it strongly to the unperturbed continuum (see Sec. I).

The emergence of the collective state at $\gamma_i > D$ is accompanied by a narrowing of the other resonances seen in the spectrum. This resulting picture looks similar to that of the perturbation theory regime of isolated resonances ($\gamma_i \ll D$). Apart from studying the positions of eigenvalues in the complex plane, one can examine the behavior of the additional phase shift $\Delta\delta$ produced in the continuous spectrum due to its interaction with the discrete states. This would enable us to see clearly how the transition from one regime to the other happens. The expression for $\Delta\delta$ can be written in the following form (analogous to one obtained in [10]):

$$\tan(\Delta\delta) = -\pi \sum_i \langle\varepsilon|W|i\rangle C_i(E), \tag{27}$$

where the continuous spectrum states are normalized as $\langle\varepsilon'|\varepsilon\rangle = \delta(\varepsilon - \varepsilon')$, and the coefficients $C_i(E)$ give the admixture of the discrete states $|i\rangle$ in the total wave function at energy E (the state $|\varepsilon\rangle$ corresponds to this energy). They satisfy the equation

$$C_i(E) = \frac{\langle i|W|\varepsilon\rangle}{E - E_i} + \frac{1}{E - E_i} \sum_j C_j(E) \times \int \frac{\langle i|W|\varepsilon'\rangle\langle\varepsilon'|W|j\rangle}{E - \varepsilon'} d\varepsilon', \tag{28}$$

where the integral in the right-hand side is the Hermitian part of Σ_{ij} (14). As we discussed at the end of Sec. II A, the latter shifts the positions of the resonances states along the real axis, and as such does not influence their widths. Thus the first term on the right-hand side of Eq. (28) can be introduced into (27), which yields

$$\tan(\Delta\delta) = -\pi \sum_i \frac{\langle\varepsilon|W|i\rangle\langle i|W|\varepsilon\rangle}{E - E_i} \tag{29}$$

or

$$\tan(\Delta\delta) = -\sum_i \frac{\gamma_i}{2(E - E_i)} .$$

This answer holds if the Hermitian part of Σ_{ij} is taken into account as well, with E_i ($|i\rangle$) replaced by the eigenvalues (eigenstates) of the matrix $E_i\delta_{ij} + \frac{1}{2}(\Sigma_{ij} + \Sigma_{ji}^*)$ [10]. It is now most straightforward to see how the narrowing occurs.

Let us assume that the number of terms in the sum on the right-hand side of Eq. (29) is finite, n. In the regime of isolated resonances, $\gamma_i \ll D$, the value of this sum is small compared to unity, except when E is close to one of the resonances, $|E - E_i| \lesssim \gamma_i$. Therefore, $\tan(\Delta\delta)$ is mainly stationary, with $\Delta\delta \approx m\pi$ (m being an integer), and it undergoes rapid rises by π when the energy E passes through each of the resonances. When the perturbation-theory widths are large, $\gamma_i \gg D$, the absolute value of the sum in Eq. (29) is almost everywhere large compared to unity, except for the values of E where

$$\sum_i \frac{\gamma_i}{E - E_i} = 0. \tag{30}$$

Clearly, this equation has $n-1$ roots $\tilde{E}_k$, one in every (E_i, E_{i+1}) interval. Between these roots the phase shift is stationary, $\Delta\delta \approx (m + \frac{1}{2})\pi$ ($|\tan(\Delta\delta)| \gg 1$), and in the vicinity of each of them $\Delta\delta$ makes a sudden jump to the next $(m + \frac{1}{2})\pi$ value, thus signaling a resonance. The larger the ratio γ/D, the more abrupt are these jumps. The extra phase

shift of $\pi/2$ is due to the broad (doorway) resonance which forms the background for narrow resonances (see below). For this reason, if the potential scattering is neglected, the cross section has maxima between the resonances, and narrow minima at the energies of the levels $\widetilde{E}_k$, where the phase shift is $m\pi$. Note that the positions of the nodes of Eq. (30) coincide with the roots of Eq. (15) for large γ_i, when the unity on the left-hand side can be neglected. Note also that the ''stationary'' smooth part of $\Delta\delta(\mathrm{mod}\pi)$ can be described by

$$\tan(\Delta\delta)\approx-\frac{\Sigma_i\gamma_i}{2(E-E_c)}=-\frac{\Gamma_c}{2(E-E_c)},$$

which is the background phase shift provided by the wide collective resonance.

It is easy to check, for the finite number of resonances n, that Eq. (27) can be rewritten in the following form [11,23]:

$$\cot(\Delta\delta)=-\frac{2(E-E_c)}{\Gamma_c}+\sum_k\frac{\Gamma_k}{2(E-\widetilde{E}_k)}, \qquad (31)$$

where E_c and Γ_c are given by (25), $\widetilde{E}_k$ are the solutions of Eq. (30), and the corresponding widths Γ_k are

$$\Gamma_k=\left[\sum_i\frac{\gamma_i}{4(\widetilde{E}_k-E_i)^2}\right]^{-1}. \qquad (32)$$

In this form the behavior of the phase shift in the $\gamma_i\gg D$ case ($\Gamma_k\ll D$) looks especially clear.

III. MODEL CALCULATIONS FOR CERIUM

In this section we would like to examine the widths of compound AIS's in a real system. As an example of such a system we take the Ce atom.

A. Spectrum of Ce

In our earlier work this atom was studied as a realistic model of a quantum chaotic system [7]. In that work the spectrum and eigenstates of the Ce atom with $J^\pi=4^-$, and 4^+ were calculated using the relativistic configuration-interaction (CI) code [24]. For the odd states the basis of many-electron states included 53 configurations corresponding to the seven nonrelativistic configurations $4f6s^25d$, $4f6s5d^2$, $4f^26s6p$, $4f6s6p^2$, $4f5d^3$, $4f5d6p^2$, and $4f^25d6p$, which produced 260 states with $J^\pi=4^-$. In spite of the moderate number of configurations the calculation produced a very dense spectrum of levels. For example, for states of $J^\pi=4^-$ symmetry, which includes the atomic ground state, the level density $\rho\simeq44.5\ \mathrm{eV}^{-1}$ was obtained for energies near the ionization threshold ($E\simeq5$ eV).

In the present work the basis set has been expanded to obtain a more realistic value of the spectral density at this energy. In particular, we have added configurations constructed from the original 53 configurations by transferring one of electrons into the next orbital, which makes a total of 121 relativistic configurations. In our calculation the spectrum of $J^\pi=4^-$ states becomes denser ($\rho\approx125\ \mathrm{eV}^{-1}$ at $E\approx5$ eV). Figure 2 compares the spectra obtained in the two calculations. It can be seen that the level structure in the lower part of the spectrum is almost unchanged, whereas at $E>4$ eV, and above the ionization threshold, the spectral density in the second calculation is indeed much higher.

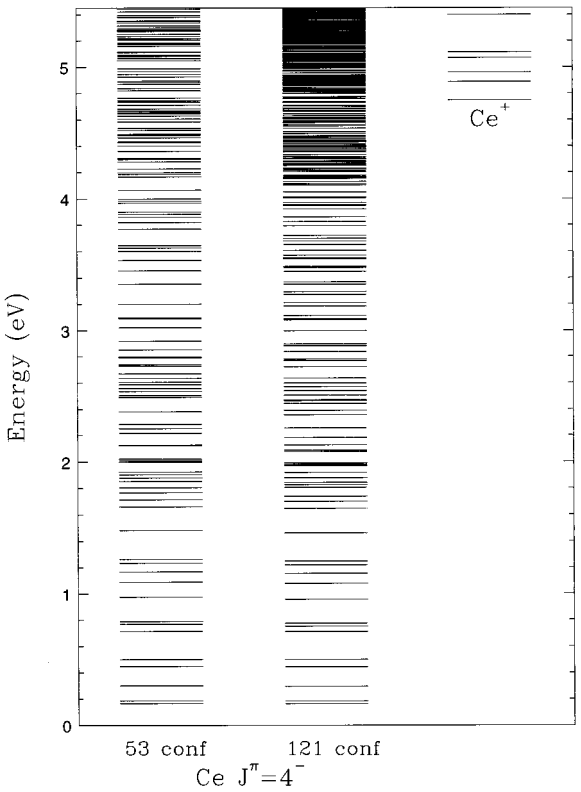

FIG. 2. Energy levels of the Ce atom with $J^\pi=4^-$ obtained in the two calculations which include 53 and 121 configurations, respectively. The third column shows the levels of the Ce^+ positive ion. Infinite Rydberg series are not presented in the graph.

Also shown in Fig. 2 is the spectrum of the lower odd levels of Ce^+ (including the $Ce^+ J^\pi=7/2^-$ ground state). These states have been obtained on the small basis which includes $4f6s^2$, $4f5d^2$, and $4f6s5d$ configurations. This calculation adequately describes the sequence of lower levels of Ce^+ and intervals between them. Thus the calculated spacing between the ground state ($J=7/2^-$) and the first excited state ($J=9/2^-$), $\Delta=0.137$ eV, is close to the experimental value, $\Delta=0.122$ eV [25]. The calculated value of the ionization potential $I=4.75$ eV is smaller than the experimental value $I=5.539$ eV. We should mention that the electron orbitals have not been optimized to obtain the best energies of the ground states of Ce and Ce^+; neither have the correlations between the valence and core electrons been taken into account in our calculation. However, this discrepancy is not very important for the model calculations we perform, since the level density of Ce does not change too much over this energy interval. Note that infinite series of Rydberg levels converging to the excited states of Ce^+ have not been included in the calculations, and they are not present in Fig. 2.

Of course, the true level density is even higher due to the presence of Rydberg series. Let us consider, for instance,

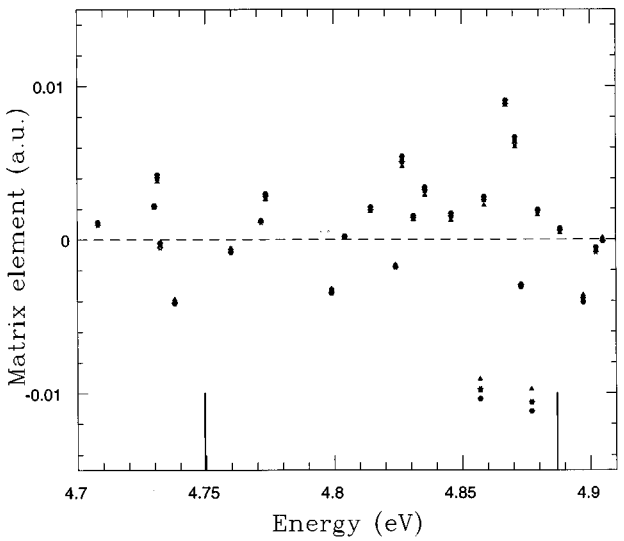

FIG. 3. Coulomb matrix elements $\nu^{3/2}\langle \mathrm{Ce}^+ ns|W|\mathrm{Ce}^* i\rangle$; solid triangles, $n=8$; solid squares, $n=9$; solid hexagons, $n=10$; and open stars, $n=11$. Thick short lines show the positions of the ground state and the first excited state of Ce^+.

such series converging to the first excited state of Ce^+. The energy of the nth Rydberg state with respect to the corresponding threshold is $E_n \simeq -1/2n^2$, and the spacing between the Rydberg levels is $D_n \simeq \partial E_n/\partial n = 1/n^3$. Then for the density $\rho^{(1)}$ of the Rydberg series of levels converging to the first excited state of Ce^+ near the ground state of Ce^+, one obtains $\rho^{(1)}=1/D_n=1/(2\Delta)^{3/2}$, where Δ is the distance between the two lowest levels of Ce^+. The density $\rho^{(k)}$ of the Rydberg series converging to the kth excited state of Ce is given by $\rho^{(k)} \simeq 1/(2k\Delta)^{3/2}$, where we assume that Δ can characterize the mean spacing between lower levels of Ce^+. To calculate the total density of the Rydberg states ρ_{Ryd}, one has to sum up all $\rho^{(k)}$:

$$\rho_{\mathrm{Ryd}}=\sum_{k=1}^{\infty}\rho^{(k)}=\sum_{k=1}^{\infty}\frac{1}{(2k\Delta)^{3/2}}=\frac{\zeta(3/2)}{(2\Delta)^{3/2}}\approx\frac{2.61}{(2\Delta)^{3/2}}\approx\frac{1}{\Delta^{3/2}}. \tag{33}$$

In order to estimate ρ_{Ryd} let us use the experimental value $\Delta \simeq 0.1$ eV, which gives $\rho_{\mathrm{Ryd}} \simeq 150\ \mathrm{eV}^{-1}$. Therefore, comparing this value with $125\ \mathrm{eV}^{-1}$ obtained in the present calculations one can see that the density of the real spectrum is at least two times higher than in our model due to the series of Rydberg states. Moreover, if we take into account the Rydberg series with different l converging to the excited states of Ce^+, which can be coupled into the same total J^π, the density of the atomic AIS may become even higher (of the order of $10^3\ \mathrm{eV}^{-1}$; this number is consistent with the experimental density of ''valence states'' near the ionization limit in U, that can be estimated from Fig. 3 of [3]).

The spectrum of Ce, or any other complex atom, consists of the two manifolds: compound AIS's and Rydberg AIS's, whose interaction with each other can be very weak. The Coulomb matrix element coupling a compound state to a Rydberg state with the principal quantum number n is reduced by the factor of $1/\sqrt{N}$, where N is the number of principal components of the compound state [see Eq. (3)], and by another factor of $n^{-3/2}$, due to the behavior of the Rydberg electron wave function at small distances. The compound AIS's are very different from the Rydberg states. The former are built of orbitals with small principal quantum numbers (such states are also called ''valence states'' [3]). Due to this fact they are relatively compact (their radius is several Bohr radii a_0), whereas the Rydberg states have large radii ($r \sim n^2 a_0$). This difference has been used by experimentalists to observe Rydberg series in lanthanides and actinides spectra [2,3]. The density of compound states is a smooth function of energy, whereas that of the Rydberg states peaks at every positive-ion threshold.

B. Decay and electromagnetic amplitudes involving compound AIS's

In what follows, AIS's lying just above the ionization threshold are examined. To restrict our consideration to one-channel decay, we study only the levels between the ground state and the first excited state of Ce^+. There are many 4^- levels of the atom lying in this energy interval (7 and 18, respectively, in the two calculations shown in Fig. 2). The AIS's we study have $J^\pi=4^-$ symmetry, and the ground state of Ce^+ has $J^\pi=7/2^-$. Therefore, the AIS's can decay via the emission of an electron with $l=0,2,4,\ldots$. However, the contribution of the s wave dominates. This is suggested, for example, by the behavior of the radial wave function in the Coulomb field ([18]),

$$R_{kl}(r) \propto \frac{(2r)^{l+1/2}}{(2l+1)!}. \tag{34}$$

The magnitude of R_{kl} at $r \sim 1$ is suppressed for $l=2,4,\ldots$. Therefore, calculating the decay of the low-lying AIS's we can consider only one continuum, $\mathrm{Ce}^+ \varepsilon s$, and the theoretical considerations of Sec. II are applicable. Of course, one can use the same formalism and take into account other decay channels as well (Appendix B).

The perturbation width of the ith AIS $|\mathrm{Ce}^* i\rangle$ is given by

$$\gamma_i = 2\pi |\langle \mathrm{Ce}^+ \varepsilon l|W|\mathrm{Ce}^* i\rangle|^2.$$

In order to calculate it one should know the wave functions of Ce in the continuum. To avoid calculating them explicitly and make do with the present CI code we use the following procedure. For low energies ε the wave function of the autoionizing electron at small distances $r \sim a_0$ is proportional to the wave function of a highly excited Rydberg state, $\psi_{\varepsilon l}(r) \simeq A_n \psi_{nl}(r)$. If $\psi_{\varepsilon l}(r)$ is normalized to the δ function of the energy, the coefficient is given by $A_n=\nu^{3/2}$, where $\nu=n-\mu$ is the effective principal quantum number, and μ is the quantum defect (see, e.g., [26]). Then we can use the substitution

$$|\mathrm{Ce}^+ \varepsilon l\rangle \rightarrow A_n |\mathrm{Ce}^+ nl\rangle, \tag{35}$$

which yields

$$\gamma_i \approx 2\pi\nu^3 |\langle \mathrm{Ce}^+ nl|W|\mathrm{Ce}^* i\rangle|^2 \quad (\nu \gg 1). \tag{36}$$

Practically, to calculate γ_i from Eq. (36) we consider the ns series with $n=$ 8–11 (the states with $n=7$ are included in the 121 configurations describing $|\mathrm{Ce}^* i\rangle$ states). The states

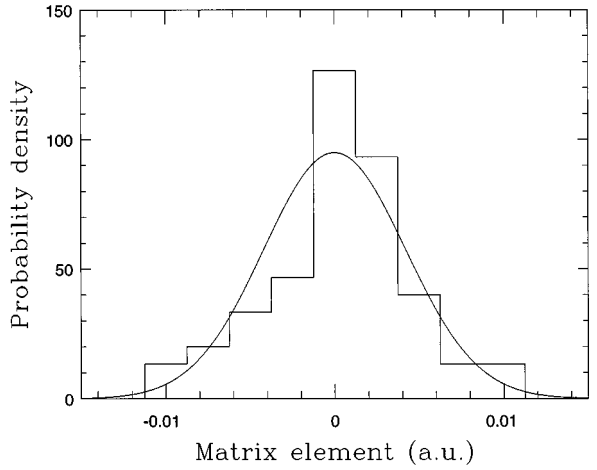

FIG. 4. Probability density of the Coulomb matrix elements $\langle \mathrm{Ce}^+ \varepsilon s|W|\mathrm{Ce}^* i\rangle$ for the 121–180 $J^\pi = 4^-$ states of Ce. The solid curve is a Gaussian distribution $(2\pi\overline{W^2})^{-1/2}\exp(-W^2/2\overline{W^2})$ with $\overline{W^2} = 1.77\times10^{-5}$ a.u. The χ^2 test for the seven central bins yields $\chi^2(6) = 5.0$.

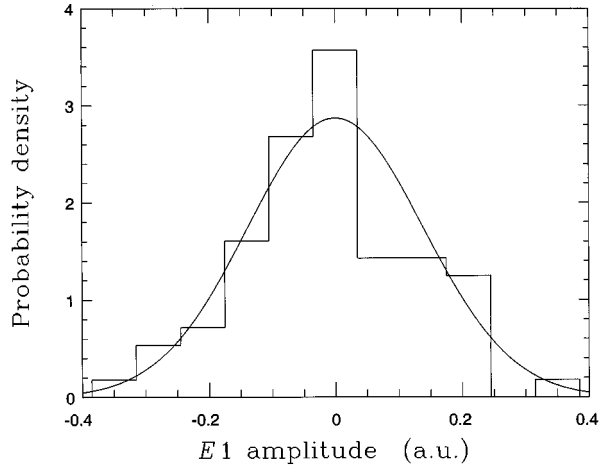

FIG. 5. Probability density of the 80 dipole matrix elements $\langle \mathrm{Ce}^* i|E1|\mathrm{Ce}4^+\rangle$ for the AIS near the ionization threshold of Ce^+. Solid line shows the Gaussian distribution with $(\overline{Q^2})^{1/2} = 0.139$. The χ^2 criterion calculated for the nine central bins of the histogram is $\chi^2(8) = 7.44$.

$|\mathrm{Ce}^* i\rangle$ are obtained by diagonalization of the Hamiltonian matrix in the basis of 121 configurations which produce 862 states with $J^\pi = 4^-$. The $|\mathrm{Ce}^+ ns\rangle$ states are eigenstates of the Hamiltonian matrix in the basis constructed by adding the Rydberg states ns to the configurations of Ce^+ mentioned above. Therefore, the lower Rydberg series $\mathrm{Ce}^+ ns$ converge to the ground state of Ce^+ shown in Fig. 2. This series is described by $E_{ns} = E_{\mathrm{Ce}^+} - 1/2(n-\mu)^2$ with $\mu \approx 4.1$. The corresponding wave functions are used to calculate the decay matrix elements $\langle \mathrm{Ce}^+ \varepsilon s|W|\mathrm{Ce}^* i\rangle$ as $\nu^{3/2}\langle \mathrm{Ce}^+ ns|W|\mathrm{Ce}^* i\rangle$. Note that the ''continuum'' and discrete states in this matrix element are orthogonal.

Figure 3 presents the Coulomb matrix elements $\nu^{3/2}\langle \mathrm{Ce}^+ ns|W|\mathrm{Ce}^* i\rangle$ calculated for different ns ($n = 8$–11). One can see that the matrix elements for different n are very close to each other. Therefore, Eq. (36) is valid, and in the further calculations we simply use the matrix elements obtained for $n = 10$.

To obtain a better understanding of the structure of the compound states in question, it is instructive to look at the statistics of their matrix elements (Fig. 4). In this figure we have plotted the probability distribution for 60 Coulomb matrix elements $\langle \mathrm{Ce}^+ \varepsilon s|W|\mathrm{Ce}^* i\rangle$ calculated for the 4^- levels 121–180 (the AIS's between the two lowest Ce^+ states are 137–154). The histogram in Fig. 4 is compared with the Gaussian distribution with variance $\overline{W^2}$. The agreement observed may not be perfect; however, it supports the theoretical reasoning that the matrix element is the sum of uncorrelated random variables and thus, obeys Gaussian statistics [Sec. I, Eq. (3) and below]. The Gaussian statistics of the matrix elements corresponds to the Porter-Thomas distribution of the widths $\gamma = 2\pi W^2$, $f(\gamma) = \exp(-\gamma/2\overline{\gamma})/\sqrt{2\pi\overline{\gamma}\gamma}$ [27]. As is known the widths of nuclear compound states are distributed according to the Porter-Thomas law [5]. The present calculation suggests that atomic compound resonances are in this respect very similar to the nuclear ones. This could be expected because the origin of the Porter-Thomas distribution is ''quantum chaos.'' Therefore, the statistics observed indicates that the compound atomic eigenstates are to a large extent chaotic, as we pointed out in [7].

The mean width of the 18 AIS's between the two lowest states of Ce^+ is $\overline{\gamma} = 2\pi\overline{W^2} = 4.3\times10^{-3}$ eV. This value must be compared with the mean level spacing $D \approx 0.008$ eV. The relation $\overline{\gamma} \approx 0.5D$ is in agreement with the estimate made in Sec. I. As discussed earlier, the density of states in our model calculation is underestimated (mainly due to the absence of Rydberg series). The following question is very important: if a better calculation (or experimental data) produce a smaller value of D, how would it change the value of $\overline{\gamma}$? Estimate (4) suggests that the decrease of D should cause a decrease of γ, as long as the residual Coulomb interaction is strong enough to mix basis components within the Γ_{spr} energy range. On the other hand, when many-electron states include electron orbitals with larger principal quantum numbers, the radius of these states increases, and the residual interaction goes down. This ultimately leads to the emergence of the two weakly interacting components in the spectrum (the compound ''valence'' states, and the Rydberg states). This transformation of the spectrum is an interesting question in its own right, deserving special investigation.

The mean width $\overline{\gamma} \approx 0.5D$ is close to the critical value $\gamma = 2D/\pi$, beyond which the regime of narrowing of resonances occurs. Therefore, the interaction of the AIS's via the continuum is important. To obtain a physical picture of how this interaction influences the shape of the resonances, we consider a process of photoionization of the lowest even state of Ce ($J^\pi = 4^+$) in the $4^+ \to 4^-$ channel. The even state of Ce has been calculated using the basis of 50 configurations in the same way as in [7]. To find the photoionization cross section we need the dipole amplitudes coupling the lowest $J^\pi = 4^+$ state to the compound states, $\langle \mathrm{Ce}^* i|E1|\mathrm{Ce}4^+\rangle$, as well as the dipole amplitude of the transition from the even state into the continuum, $\langle \mathrm{Ce}^+ \varepsilon s|E1|\mathrm{Ce}4^+\rangle$. The latter was calculated as $\nu^{3/2}\langle \mathrm{Ce}^+ ns|E1|\mathrm{Ce}4^+\rangle$, which gave a numerical value of 0.375.

The calculated dipole amplitudes give us another possibility to analyze the statistical properties of the compound states. In Fig. 5 we present the distribution of the $E1$ amplitudes $\langle \mathrm{Ce}^* i|E1|\mathrm{Ce}4^+\rangle \equiv Q_i$ for 80 compound states near the ionization threshold. The root-mean-square value of these matrix elements is $\sqrt{\overline{Q_i^2}} = 0.178$. The histogram in Fig. 5 is in reasonable agreement with the Gaussian fit drawn to minimize χ^2. Thus the line strengths Q_i^2 involving compound states should have a Porter-Thomas distribution. Earlier evidence of this effect and the results of calculations of dipole excitations in complex atoms can be found in [28]. At a closer inspection one may notice some similarities in the deviations of the histograms from the Gaussians in Figs. 4 and 5, particularly an abundance of small matrix elements. We believe that this can be explained (as in [7], Fig. 17) as traces of broken symmetries (the total spin and the total orbital angular momentum), not completely removed by the spin-orbit interaction. Another reason for the Gaussian statistics to be distorted can be the presence of states with very different mean radii whose mixing by the residual interaction is not complete. This effect becomes dominating when higher Rydberg states are considered together with the compound valence states.

Estimating the dipole amplitude in the spirit of Eq. (4), we obtain

$$\langle \mathrm{Ce}^* i|E1|\mathrm{Ce}4^+\rangle \sim Q_0\left(\frac{q'}{N}\right)^{1/2}, \tag{37}$$

where q' is the number of single-particle transitions which contribute to the many-particle matrix element, and Q_0 is a typical single-particle dipole matrix element between valence and nearby excited orbitals ($Q_0 \sim 1$). Since we consider the lowest even state of Ce (with the dominant configuration $4f^2 6s^2$), there are few such transitions, e.g., $4f \to 5d, 6s \to 6p$, which gives, say, $q' \sim 5$. Therefore, for $N \sim \Gamma_{\mathrm{spr}}/D \sim 200$, estimate (37) gives $Q_i \sim 0.1$, in accord with the root-mean-squared value 0.178. Estimate (37) shows also that the oscillator strengths $f_i \propto Q_i^2$ are inversely proportional to N. This fact is a manifestation of the dipole sum rule, $\Sigma_i f_i \approx n_e$ (n_e is the number of active electrons), as the number of transitions from a given state into the compound spectrum of states is proportional to N. More precise estimates of the mean-square amplitudes involving compound states can be obtained using statistical theory [7].

C. Interaction of compound AIS's via the continuum

To elucidate the effects produced by the interaction of AIS's via the continuum we, first, calculate the photoabsorption spectrum as a sum of Lorentzian profiles,

$$\sum_i \frac{\gamma_i}{2\pi} \frac{Q_i^2}{(E-E_i)^2 + \gamma_i^2/4}, \tag{38}$$

i.e., neglecting the interaction of the AIS's [29]. Figure 6(a) presents the result of this calculation. Due to fluctuations of level positions and widths a picture of isolated resonances is observed on the left-hand side of the energy scale, where the resonance widths are smaller than the level spacings. Conversely, there are wide overlapping resonances on the right-hand side of Fig. 6(a).

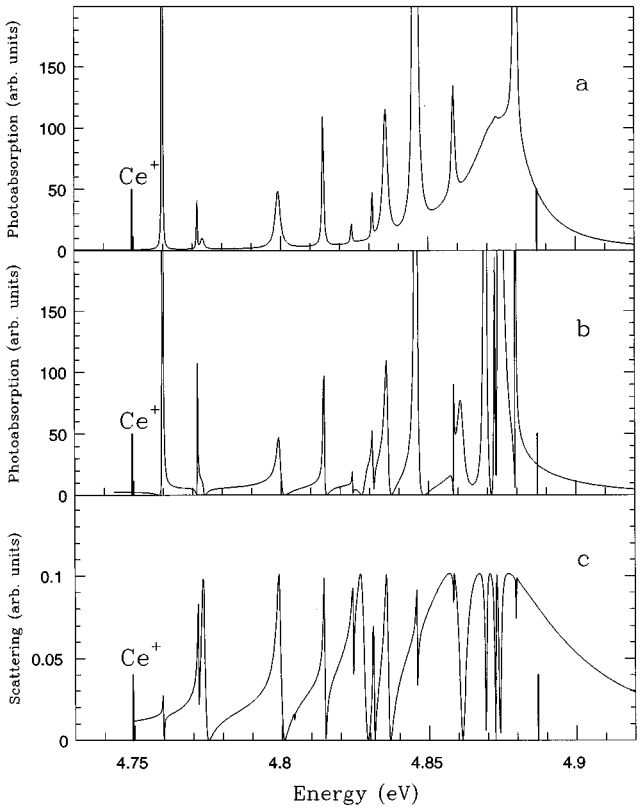

FIG. 6. (a) Photoabsorption spectrum obtained as $\Sigma_i(\gamma_i/2\pi)\, f_i/[(\omega - E_i)^2 + \gamma_i^2/4]$, where f_i is the oscillator strength. (b) Photoabsorption spectrum calculated with AIS interaction via the continuum included. (c) Electron-Ce^+ scattering (resonance approximation). The energy is given with respect to the Ce ground state. Thick lines indicate the positions of the two lowest states of Ce^+.

The photoabsorption amplitude which takes into account the interaction of AIS's is given by Eq. (12). In our calculations we have neglected the real part of Σ, Eq. (14), because the principal value of the integral is quite small due to a very weak dependence of the matrix elements $\langle i|W|\varepsilon'\rangle$ on ε' (this can be seen from Fig. 3). The photoabsorption cross section $|A(E)|^2$ [29] is presented in Fig. 6(b). It is quite natural that the left-hand part of the spectrum is almost unchanged in comparison with Fig. 6(a). Due to the narrowness of the resonances in this part of the spectra their interaction via the continuum do not change their widths. Conversely, on the right-hand side of the picture dramatic changes are obvious. The local mean perturbation width here turns out to be greater than the local mean level spacing. As a result, very sharp resonances become the main feature of the spectrum. Their total width is apparently smaller than that of the broad feature in Fig. 6(a). This is a manifestation of the regime of narrowing described in Sec. II B.

If the narrowing takes place then one should expect a wide collective (doorway) state to emerge. However, such a resonance is not visible in the spectrum. The point is that, while acquiring width, the doorway state does not obtain a larger share of the oscillator strength (unless the $E1$ and

decay amplitudes are correlated in some way, which may produce a ''giant resonance'' [5,14]). In other words, it does not work as the doorway for the absorption of the photon. However, the doorway state has the strongest coupling to the continuum. Thus it becomes the main feature of the electron-ion scattering cross section in the given continuous channel. Using the notation of Eq. (12) we can write the resonant part of the electron-ion scattering amplitude as

$$T(E)=W^{+}(\Delta-\Sigma)^{-1}W. \tag{39}$$

If the contribution of potential scattering is neglected, the cross section is simply proportional to $|T(E)|^2$. This quantity is plotted in Fig. 6(c). The contribution of each of the resonances is now determined only by its coupling to the continuum. Therefore, we observe narrower and weaker, or wider and stronger features. The doorway state reveals itself as a broad structure on the right-hand side of Fig. 6(c). Within its range the narrow resonances appear as sharp dips on the broad-scale background. This picture is in a striking contrast with the photoabsorption cross section, where direct photoabsorption into the continuum is simply too small to give a noticeable background.

Of course, the calculations presented in this section are not realistic in the sense that they can reproduce some particular features of the real photoabsorption spectrum of Ce. However, they use the decay and $E1$ amplitudes from the realistic CI calculations, which are in agreement with theoretical estimates (3) and (37). Most importantly, the calculations indicate that the perturbation widths of the AIS's are comparable to their level spacing. This, on one hand, makes atomic compound states observable, and, on the other hand, brings about the interesting regime of narrowing. It is quite important that if more than one continuum is taken into account, the role of the interaction of AIS's via the continuum is still determined by the magnitude of the *partial* width in comparison with D (Appendix B). Therefore, such an interaction and the effects it produces (narrowing and ''collectivization,'' or, formation of doorway states) are likely to be important in the many-channel case as well.

IV. CONCLUSIONS

The prime motivation of the present work is to study the spectrum of complex open-shell atoms above the ionization threshold, and to find out whether it is possible to observe compound atomic resonances in this region. We have shown that simultaneous excitation of several valence electrons in atoms produces a dense spectrum of compound AIS's. The statistics of matrix elements involving compound states are close to Gaussian. The root-mean-square estimates of the matrix elements can be made in terms of the number of principal components of the compound states.

We have demonstrated, both analytically and numerically, that the interaction of compound states via the continuum results in the overall narrowing of the resonances, accompanied by the formation of broad collective resonant states (doorway states). The narrow resonances are probably best observed in photoabsorption and photoionization experiments, whereas the doorway states should feature in electron-ion scattering. We believe that the effects discussed in the present paper can be found in almost any atom at energies sufficient for excitation of several electrons above the ground state. High-resolution atomic photoionization measurements provide growing experimental evidence for this (see, e.g., [30]).

The effects produced by the interaction of compound AIS's via the continuum can also be important for the problem of dielectronic recombination, which is believed to play an essential role in high-temperature plasmas (see, e.g., review [31]). Such effects can be driven by an external electric field. Even if the direct field ionization does not take place, mixing of different state manifolds varies the level spacings and the AIS decay amplitudes [32]. The effect of narrowing may influence the $1/n^4$ scaling of the widths of autoionizing Rydberg states observed in strong electric fields [33]. One can only imagine what kind of reach physics will be involved if an external electric or magnetic field is applied to such systems (dynamical enhancement of perturbations in weak fields, transition from regular states to chaos and ''collectivization'' in stronger fields, etc.).

There is also another question we have merely touched upon in this work. It concerns the interaction of compound ''valence'' states with Rydberg level series in complex open-shell atoms. So far there is no criteria or condition which would tell at what n the perturbation of the Rydberg series becomes weak.

Finally, the existence and manifestations of quantum chaos in many-electron atoms remains largely an unexplored field. Apart from its fundamental importance, such a point of view may prove to be useful for studying complex atoms where accurate calculations employing even the most sophisticated numerical methods will remain for a while a formidable task.

ACKNOWLEDGMENTS

The authors would like to thank O. P. Sushkov, M. Yu. Kuchiev, and M. G. Kozlov for useful discussions, and gratefully acknowledge the support of the Australian Research Council.

APPENDIX A: PERTURBATION THEORY AND EMERGENCE OF THE COLLECTIVE STATE

To obtain a better understanding of the model with n equally spaced levels E_i and constant coupling to the continuum, $\Sigma_{ij}=-i\gamma/2$, studied in Sec. II B, it is instructive to apply perturbation theory to find the positions and widths of the resonances. Since the potential Σ in this model is purely imaginary, the odd-order perturbation terms contribute to the width, whereas the even ones shift the resonance along the real axis. The three lowest-order corrections to the energy of the kth resonance are

$$\Delta E_k^{(1)}=-i\frac{\gamma}{2}, \quad \Delta E_k^{(2)}=-\frac{\gamma^2}{4}{\sum_l}' \frac{1}{E_k-E_l}, \tag{A1}$$

$$\Delta E_k^{(3)}=i\frac{\gamma^3}{8}\left[{\sum_{lm}}' \frac{1}{(E_k-E_l)(E_k-E_m)}-{\sum_l}' \frac{1}{(E_k-E_l)^2}\right], \tag{A2}$$

where in the primed sums $l,m\neq k$. If the number of levels is large ($n\gg 1$) the sums in Eqs. (A1) and (A2) can be estimated as follows:

$$\sum{}' \frac{1}{E_k-E_l}\simeq\frac{1}{D}\ln\left(\frac{\frac{n}{2}+k}{\frac{n}{2}-k}\right),$$

$$\sum{}' \frac{1}{(E_k-E_l)^2}\simeq\frac{2}{D^2}\zeta(2)=\frac{\pi^2}{3D^2},$$

where we assumed that the levels are distributed symmetrically with respect to $E=0$, $-n/2<k<n/2$, i.e., $k=0$ corresponds to the center of the spectrum. Thus the resonance is shifted with respect to E_k by

$$\Delta E_k\simeq-\frac{\gamma^2}{4}\ln\left(\frac{\frac{n}{2}+k}{\frac{n}{2}-k}\right), \tag{A3}$$

and its width is

$$\Gamma_k\simeq\gamma-\frac{\gamma^3}{4D^2}\left\{\left[\ln\left(\frac{\frac{n}{2}+k}{\frac{n}{2}-k}\right)\right]^2-2\zeta(2)\right\}. \tag{A4}$$

For resonances in the middle of the spectrum, $|k|\ll n/2$, hence $\ln(\,)\ll 1$, the shift ΔE_k is very small, and the widths are larger than the first-order estimate γ, due to the third-order correction in brackets. Note that the perturbation theory parameter for these states is γ/D. Near the edges of the spectrum, $|(n/2)-k|\ll n/2$, or $|(n/2)+k|\ll n/2$, the logarithm becomes large, $|\ln(\,)|\simeq\ln n\gg 1$, and the third-order term makes the widths smaller than γ. The perturbation-theory parameter for these states is $\gamma\ln n/D$, and the perturbation series expansion breaks down at much smaller γ/D. Moreover, even for arbitrary small γ/D one can find n for which the perturbation theory fails near the edges of the spectrum (although such n will have to be exponentially large). The results obtained in the numerical example, Fig. 1, clearly illustrate all these effects.

For $\gamma/D\gtrsim 1$ the perturbation theory becomes invalid everywhere. This corresponds to the regime of narrowing of resonances, and to the emergence of the collective state which absorbs most of the total width. It is interesting that the width of the collective state can be calculated on weaker assumptions than those used to derive the result of Eq. (20). Consider Eq. (16b), and assume that Γ is greater than D. The expression under the sum is then a smooth function of E_i, and can be replaced by the integral

$$\sum_i\frac{\gamma_i}{(E-E_i)^2+\Gamma^2/4}\simeq\frac{\gamma}{D}\int_{-nD/2}^{nD/2}\frac{dE_i}{(E-E_i)^2+\Gamma^2/4}$$

$$=\frac{4\gamma}{\Gamma D}\tan^{-1}\frac{nD}{\Gamma}, \tag{A5}$$

where we put $E=0$ in the last expression, since the collective state emerges from the middle of the spectrum. Introducing (A5) into Eq. (16b), we obtain the expression for the width of the collective state valid for $\Gamma\gg D$ [15]:

$$\Gamma=nD\,\cot(D/\gamma). \tag{A6}$$

Note that the above derivation is still valid for $\gamma_i\neq$ const, and fluctuating level positions. In this case γ in Eq. (A6) should be replaced with $\overline{\gamma}$, and D with the mean level spacing. Equation (A6) shows that for $n\gg 1$ the transformation of the spectrum happens quite rapidly, which prompted the authors of [15] to call it a ''phase transition.'' It is also interesting to observe that formally the collective state width (A6) turns into zero at $D/\gamma=\pi/2$, which coincides with the critical condition for the picket-fence model, Sec. II B.

APPENDIX B: MANY-CHANNEL PROBLEM

It is very straightforward to generalize the formalism of Sec. II A to the case of n discrete states coupled to K different continua. Let $|\varepsilon_k\rangle$ be the state of the system in the kth continuum ($k=1,\ldots,K$). The discrete state i is coupled to the kth continuum by the matrix element $W_{ik}=\langle i|W|\varepsilon_k\rangle$, so W_{ik} is now a $n\times K$ matrix. If we are concerned with the photoabsorption from the $|g\rangle$ state, we should introduce K electromagnetic amplitudes $d_k=\langle\varepsilon_k|\hat{d}|g\rangle$. Now the vector $A(E)$ of photoabsorption amplitudes $A_k(E)$ in the kth channel can be presented in complete analogy with Eq. (9) by the perturbation series expansion

$$A(E)=d+W^\dagger\chi Q+W^\dagger\chi\widetilde{Q}+W^\dagger\chi\Sigma\chi Q+W^\dagger\chi\Sigma\chi\widetilde{Q}+\cdots, \tag{B1}$$

where the definitions of the n-component vector $\widetilde{Q}_i$ and $n\times n$ matrix Σ_{ij} are modified with respect to Eqs. (10) and (11) by the extra summation over the channels,

$$\widetilde{Q}_i=\sum_k\int\frac{\langle i|W|\varepsilon_k'\rangle\langle\varepsilon_k'|\hat{d}|g\rangle}{E-\varepsilon_k'+i\delta}d\varepsilon_k', \tag{B2}$$

$$\Sigma_{ij}=\sum_k\int\frac{\langle i|W|\varepsilon_k'\rangle\langle\varepsilon_k'|W|j\rangle}{E-\varepsilon_k'+i\delta}d\varepsilon_k'. \tag{B3}$$

The resulting photoabsorption amplitude is given in the closed form identical to Eq. (12),

$$A(E)=d+W^\dagger(\Delta-\Sigma)^{-1}[Q+\widetilde{Q}], \tag{B4}$$

and the total photoabsorption cross section is proportional to $A^\dagger(E)A(E)=\Sigma_k|A_k(E)|^2$.

The poles of the amplitude (B4) are determined by the eigenvalues of Eq. (13), and widths of the resonances corresponding to these poles are due to the presence of an imaginary part in the matrix Σ_{ij},

$$\Sigma_{ij}=\sum_k\int\frac{\langle i|W|\varepsilon_k'\rangle\langle\varepsilon_k'|W|j\rangle}{E-\varepsilon_k'}d\varepsilon_k'$$

$$-i\pi\sum_k\langle i|W|\varepsilon_k\rangle\langle\varepsilon_k|W|j\rangle, \tag{B5}$$

where, as in Eq. (14), the integrals are calculated in the principal value sense. If perturbation theory is applicable, then $\gamma_i^k = 2\pi|W_{ik}|^2$ is the partial width of the ith resonance associated with the kth channel, and the total perturbation width of this AIS is given by the sum $\gamma_i = \Sigma_k \gamma_i^k$ If the partial widths for different channels are of the same order of magnitude, the condition for nonoverlapping resonances is now $\overline{\gamma_{\rm part}} K \ll D$, where $\overline{\gamma_{\rm part}}$ is the average partial width of the AIS.

The imaginary part of Σ_{ij} is now the sum of separable terms. It is easy to show that if we neglect its real part (or, if we diagonalize it prior to the inclusion of the imaginary part, and thus incorporate the corresponding energy shifts in the ''unperturbed'' energies E_i), the poles of the amplitude in the complex energy plane will be solutions of the algebraic equation. Indeed, let us introduce $\Sigma_{ij} = -i\pi\Sigma_k W_{ik} W_{kj}$ into Eq. (13):

$$(E - E_i) C_i + i\pi \sum_k W_{ik} \sum_j W_{kj} C_j = 0. \tag{B6}$$

Denoting $\Sigma_j W_{kj} C_j \equiv F_k$, one can easily obtain an equation for F_k,

$$F_l + i\pi \sum_k \left[\sum_i \frac{W_{li} W_{ik}}{E - E_i} \right] F_k = 0. \tag{B7}$$

The solvability condition for this homogeneous equation is

$$\det\left(\delta_{km} + i\pi \sum_i \frac{W_{ki} W_{im}}{E - E_i} \right) = 0, \tag{B8}$$

where the rank of the matrix in brackets is K. This equation generalizes the single-channel equation (15). It gives the positions of poles of the S matrix in the complex plane [11], and its alternative derivations can be found in [13,14,16].

Generally, in the K-channel case there are K collective short-lived states (doorways) that emerge in the regime of strongly interacting resonances, whereas the widths of the rest of $n-K$ states are suppressed [12–14,16,20]. In the extreme case when the collective state widths are much greater than the energy spanned by E_i on the real axis ($\overline{\gamma_{\rm part}} \gg D$), the widths of the collective states are found from the characteristic equation

$$\det\left(\Gamma \delta_{km} - 2\pi \sum_i W_{ki} W_{im} \right) = 0, \tag{B9}$$

which follows from Eq. (B8) if we replace $E \to E - i\Gamma/2$, and neglect $|E - E_i|$ as small compared to Γ. There are exactly K short-lived doorway states if all K rows of the matrix W_{ki} are linearly independent, in other words, if the K vectors $\mathbf{W}_k = (W_{k1}, \ldots, W_{kn})$ in n-dimensional space form a K-dimensional subspace. Otherwise, Eq. (B9) has solutions $\Gamma = 0$, and the number of doorway states is less than K. It is equal to the number of linearly independent $\mathbf{W}_k$. The configuration of K vectors $\mathbf{W}_k$ in space, and hence the behavior of the system in the strongly interacting resonance regime, can be characterized by the $K(K-1)/2$ independent elements of the ''overlap matrix'' [11]

$$O_{km} = 2\pi \sum_i W_{ki} W_{im} / \sqrt{\gamma_k^{(c)} \gamma_m^{(c)}}, \tag{B10}$$

where $\gamma_k^{(c)} = 2\pi\Sigma_i |W_{ki}|^2$ is the total width associated with the kth channel. The matrix elements (B10) are in fact equal to $\cos\Theta_{km}$, where Θ_{km} is the angle between $\mathbf{W}_k$ and $\mathbf{W}_m$ (these parameters were used in [13,14]).

Let us consider $n \gg 1$ *compound* AIS's embedded in K continua. Due to the chaotic nature of the compound states, the decay amplitudes W_{ki} for them are uncorrelated Gaussian variables (this assumption was used when studying the distribution of widths in matrix models [20,21]). The root-mean-square estimate of the sum in Eq. (B10) then yields $O_{km} \sim 1/\sqrt{n}$ $(k \neq m)$. This means that the off-diagonal matrix elements are small, and the vectors $\mathbf{W}_k$ are almost orthogonal to each other. In this case there is a doorway state in each of the K channels (for $\overline{\gamma_{\rm part}} \gg D$), and the channels become effectively decoupled from each other. To show this formally, let us introduce the complex energy $E - i\Gamma/2$ into Eq. (B8) explicitly, and expand the corresponding matrix in inverse powers of Γ,

$$\begin{aligned} &\delta_{km} + i\pi \sum_i W_{ki} W_{im} (E - i\Gamma/2 - E_i)^{-1} \\ &\quad = \delta_{km} - \frac{2\pi}{\Gamma} \sum_i W_{ki} W_{im} + \frac{4\pi i}{\Gamma^2} \sum_i W_{ki} W_{im} (E - E_i) \\ &\qquad + \frac{8\pi}{\Gamma^3} \sum_i W_{ki} W_{im} (E - E_i)^2 + \cdots. \end{aligned}$$

As explained above, the off-diagonal matrix elements are suppressed, and hence can be neglected. Retaining all terms up to Γ^{-3} we obtain, instead of Eq. (B8);

$$\prod_{k=1}^{K} \left[1 - \frac{1}{\Gamma} \sum_i \gamma_i^k + \frac{2i}{\Gamma^2} \sum_i \gamma_i^k (E - E_i) + \frac{4}{\Gamma^3} \sum_i \gamma_i^k (E - E_i)^2 \right] = 0. \tag{B11}$$

Thus we immediately obtain the positions and widths of the K doorway states:

$$E_k^{(c)} = \frac{\Sigma_i \gamma_i^k E_i}{\Sigma_i \gamma_i^k}, \tag{B12}$$

$$\Gamma_k^{(c)} \simeq \gamma_k^{(c)} - \frac{4}{[\gamma_k^{(c)}]^2} \sum_i \gamma_i^k (E_k^{(c)} - E_i)^2, \tag{B13}$$

in direct analogy with Eqs. (20) and (21). Each of the doorway states accumulates almost all width in the corresponding channel ($\Gamma_k^{(c)} \approx n\overline{\gamma_{\rm part}}$). The second term on the right-hand side of Eq. (B13) enables one to estimate the average widths of the $n-K$ narrow resonances [see Eqs. (22) and (23)]:

$$\overline{\Gamma}_{\text{narrow}}=\frac{1}{n-K}\sum_{k}\frac{4}{[\gamma_k^{(c)}]^2}\sum_{i}\gamma_i^k(E_k^{(c)}-E_i)^2\simeq\frac{KD^2}{3\overline{\gamma}_{\text{part}}}. \tag{B14}$$

Note that the condition for the emergence of the doorway states in the many-channel case is $\overline{\gamma}_{\text{part}}\gg D$.

Therefore, in the K-channel case one should distinguish the following four regimes: (i) $\overline{\gamma}_{\text{part}}<D/K$, a perturbation-theory regime, yielding a spectrum of isolated resonances with widths $\Gamma_i=\Sigma_k\gamma_i^k$. (ii) $D/K<\overline{\gamma}_{\text{part}}<D$, a perturbation-theory regime, yielding a picture of overlapping noninteracting or weakly interacting resonances in the spectrum. (iii) $D<\overline{\gamma}_{\text{part}}<KD$, a nonperturbative regime (formation of collective states, or doorways, and narrowing) takes over; however, the widths of the narrow resonances (B14) are still greater than the mean level spacing. (iv) $\overline{\gamma}_{\text{part}}>KD$, the regime of extreme narrowing; isolated narrow resonances again become the main feature of the spectrum. This picture and estimates (B13) and (B14) are in agreement with the results of numerical modeling [20]. Note that regimes (ii) and (iii) leave enough room for the existence of Ericson's fluctuations, which take place in spectra when the state widths are uncorrelated and greater than the level spacing [34] (see also [15]).

[1] W. C. Martin, R. Zabulas, and L. Hagan, *Atomic Energy Levels—The Rare-Earth Elements*, Natl. Bur. Stand. Ref. Data Ser., Natl. Bur. Stand. (U.S.), Circ. No. 60 (U.S., GPO, Washington, DC, 1978).

[2] J. A. Paisner, R. W. Solarz, and E. F. Worden, in *Laser Spectroscopy III*, edited by J. L. Hall and J. L. Carlsten (Springer-Verlag, Berlin, 1977), p. 160.

[3] R. W. Solarz, C. A. May, L. A. Carlson, E. F. Worden, S. A. Johnson, J. A. Paisner, and L. J. Radziemski, Jr., Phys. Rev. A **14**, 1129 (1976).

[4] J. P. Connerade, M. A. Baig, and M. Sweeney, J. Phys. B **23**, 713 (1990).

[5] A. Bohr and B. Mottelson, *Nuclear Structure* (Benjamin, New York, 1969), Vol. 1.

[6] H. S. Camarda and P. D. Georgopulos, Phys. Rev. Lett. **50**, 492 (1983).

[7] V. V. Flambaum, A. A. Gribakina, G. F. Gribakin, and M. G. Kozlov, Phys. Rev. A **50**, 267 (1994).

[8] O. P. Sushkov and V. V. Flambaum, Usp. Fiz. Nauk **136**, 3 (1982) [Sov. Phys. Usp. **25**, 1 (1982)].

[9] U. Griesmann, N. Shen, J. P. Connerade, K. Sommer, and J. Hormes, J. Phys. B. **21**, L83 (1988).

[10] U. Fano, Phys. Rev. **124**, 1866 (1961).

[11] F. H. Mies, Phys. Rev. **175**, 164 (1968). This early work presented the formalism of many-resonance–many-channel theory, introduced the overlap matrix, and examined the effect of interacting resonances (including narrowing) for various atomic and molecular models.

[12] P. Kleinwächter and I. Rotter, Phys. Rev. C **32**, 1742 (1985), observed the emergence of a collective short-lived state in numerical simulations of nuclear reactions.

[13] An extensive study of the problem including statistical properties of the resonance energies and widths is presented in V. V. Sokolov and V. G. Zelevinsky, Phys. Lett. B **202**, 10 (1987); Nucl. Phys. A **504**, 562 (1989). They also pointed out that the collective state in optics is known as the Dicke state, [R. H. Dicke, Phys. Rev. **93**, 99 (1954)].

[14] V. V. Sokolov and V. G. Zelevinsky, Fizika (Zagreb) **22**, 303 (1990).

[15] V. V. Sokolov and V. G. Zelevinsky, Ann. Phys. **216**, 323 (1992).

[16] V. B. Pavlov-Verevkin, Phys. Lett. A **129**, 168 (1988); A. V. Churakov, T. Yu. Mikhailova, V. B. Pavlov-Verevkin, and V. I. Pupyshev, *ibid.* A **144**, 86 (1990); F. Remacle, M. Munster, V. B. Pavlov-Verevkin, and M. Desouter-Lecomte, *ibid.* **145**, 265 (1990).

[17] The effect of the energy dependence is considered in a model case by M. Desouter-Lecomte, J. Liévin, and V. Brems, J. Chem. Phys. **103**, 4523 (1995).

[18] L. D. Landau and E. M. Lifshits, *Quantum Mechanics: Non-Relativistic Theory* (Pergamon, Oxford, 1965).

[19] N. F. Mott and H. S. W. Massey, *The Theory of Atomic Collisions* (Clarendon, Oxford, 1965).

[20] K. Someda, H. Nakamura, and F. H. Mies, Chem. Phys. **187**, 195 (1994).

[21] N. Lehmann, D. Saher, V. V. Sokolov, and H.-J. Sommers, Nucl. Phys. A **582**, 223 (1995).

[22] I. S. Gradshtein and I. M. Ryzhik, *Tables of Integrals, Series and Products* (Academic, New York, 1980).

[23] E. P. Wigner, Ann. Math. **53**, 36 (1951).

[24] V. F. Brattsev, G. B. Deineka, and I. I. Tupitsyn, Izv. Akad. Nauk Ser. Fiz. [Bull. Acad. Sci. USSR, Phys. Ser. (USA) **41**, 173 (1977)]; S. A. Kotochigova and I. I. Tupizin, J. Phys. B **20**, 4759 (1987).

[25] A. A. Radtsig and B. M. Smirnov, *Parameters of Atoms and Atomic Ions: Handbook* (Energoatomizdat, Moscow, 1986).

[26] U. Fano and J. W. Cooper, Phys. Rev. **137**, A1364 (1965).

[27] C. E. Porter and R. G. Thomas, Phys. Rev. **104**, 483 (1956).

[28] R. Karazija, *Sums of Atomic Quantities and Mean Characteristics of Spectra* (Mokslas, Vilnius, 1991).

[29] In Eq. (38) and in the calculation of the photoabsorption cross section, we drop the standard factor proportional to the photon energy, which changes very little in the energy range considered.

[30] J. P. Connerade, M. A. Baig, and M. Sweeney, J. Phys. B **23**, 713 (1990).

[31] L. J. Roszman, in *Physics of Electronic and Atomic Collisions*, edited by S. Datz (North-Holland, Amsterdam, 1982), p. 641.

[32] The spectrum of AIS states of Ba is probably still too simple, and excitations of three or more electrons have to be considered. Nevertheless, strong effects observed in the calculations of D. J. Armstrong and C. H. Greene, Phys. Rev. A **50**, 4956 (1994), particularly some peculiarities in the statistics of the AIS widths, indicate the presence of an interesting problem.

[33] S. M. Jaffe, R. Kachru, N. H. Tran, H. B. van Linden van den Heuvell, and T. F. Gallagher, Phys. Rev. A **30**, 1828 (1984).

[34] T. E. O. Ericson, Phys. Lett. **23**, 97 (1966); T. Ericson and T. Mayer-Kuckuk, Ann. Rev. Nucl. Sci. **16**, 183 (1966).